

# Bone Marrow Transplantation Transfers Age-Related Susceptibility to Neovascular Remodeling in Murine Laser-Induced Choroidal Neovascularization

Diego G. Espinosa-Heidmann,<sup>1</sup> Goldis Malek,<sup>2</sup> Priyatham S. Mettu,<sup>1</sup> Alejandro Caicedo,<sup>3</sup> Peter Saloupis,<sup>1</sup> Sarah Gach,<sup>1</sup> Askia K. Dunnon,<sup>1</sup> Peng Hu,<sup>1</sup> Maria-Grazia Spiga,<sup>1</sup> and Scott W. Cousins<sup>1</sup>

<sup>1</sup>The Duke Center for Macular Diseases, Duke Eye Center, Durham, North Carolina

<sup>2</sup>Albert Eye Research Institute, Department of Ophthalmology, Duke University, Durham, North Carolina

<sup>3</sup>Bascom Palmer Eye Institute, Department of Ophthalmology, University of Miami Miller School of Medicine, Miami, Florida

Correspondence: Scott W. Cousins, Duke Center for Macular Diseases, Duke Eye Center, 2351 Erwin Road, Durham, NC 27705; [scott.cousins@duke.edu](mailto:scott.cousins@duke.edu)

DGE-H and GM contributed equally to the work presented here and should therefore be regarded as equivalent authors.

Submitted: June 5, 2013  
Accepted: October 9, 2013

Citation: Espinosa-Heidmann DG, Malek G, Mettu PS, et al. Bone marrow transplantation transfers age-related susceptibility to neovascular remodeling in murine laser-induced choroidal neovascularization. *Invest Ophthalmol Vis Sci.* 2013;54:7439-7449.  
DOI:10.1167/iovs.13-12546

**PURPOSE.** Neovascular remodeling (NVR), the progression of small capillaries into large-caliber arterioles with perivascular fibrosis, represents a major therapeutic challenge in neovascular age-related macular degeneration (AMD). Neovascular remodeling occurs after laser-induced choroidal neovascularization (CNV) in aged but not young mice. Additionally, bone marrow-derived cells, including macrophages, endothelial precursor cells, and mesenchymal precursor cells, contribute to CNV severity. In this study, we investigated the impact of aged bone marrow transplantation (BMT) on the degree of fibrosis, size, and vascular morphology of CNV lesions in a mouse model of laser-induced CNV.

**METHODS.** Young (2 months) and old (16 months) mice were transplanted with green fluorescent protein (GFP)-labeled bone marrow isolated from either young or old donors. Laser CNV was induced 1 month following transplant, and eyes were analyzed via choroidal flat mounts and immunohistochemistry 1 month postlaser. The identity of cells infiltrating CNV lesions was determined using specific markers for the labeled transplanted cells (GFP+), macrophages (F4/80+), perivascular mesenchymal-derived cells (smooth muscle actin, SMA+), and endothelial cells (CD31+).

**RESULTS.** Bone marrow transplantation from aged mice transferred susceptibility to NVR into young recipients. Inversely, transplantation of young marrow into old mice prevented NVR, preserving small size and minimal fibrosis. Mice with NVR demonstrated a greater relative contribution of marrow-derived SMA+ perivascular mesenchymal cells as compared to other cells.

**CONCLUSIONS.** Our findings indicate that the status of bone marrow is an important determining factor of neovascular severity. Furthermore, we find that perivascular mesenchymal cells, rather than endothelial cells, derived from aged bone marrow may contribute to increased CNV severity in this murine model of experimental neovascularization.

**Keywords:** age-related macular degeneration, experimental choroidal neovascularization, bone marrow-derived perivascular precursor cells, bone marrow transplantation, neovascular remodeling

Persistent disease activity in spite of anti-vascular endothelial growth factor (VEGF) therapy remains a major unmet therapeutic need in the treatment of neovascular age-related macular degeneration (AMD), affecting up to 50% of treated eyes.<sup>1</sup> Persistent disease activity includes not only residual intra- or subretinal fluid, but also enlargement of choroidal neovascularization (CNV), formation of large-caliber branching arterioles, and perivascular fibrosis. These features resemble the experimental process of neovascular remodeling (NVR), the progression of small capillaries into large-caliber arterioles with perivascular fibrosis.<sup>2</sup> Neovascular remodeling can be induced in the laser CNV model under various conditions, including after exposure of mice to cigarette smoke or systemic inflammatory toxins (Ref. 3 and Espinosa-Heidmann DG, et al. *IOVS* 2007;48:ARVO E-Abstract 6017). However, NVR occurs

after laser-induced CNV in aged mice without additional manipulation. In contrast, unmanipulated young mice develop small lesions with mostly capillaries and minimal fibrosis.<sup>4</sup>

Pathological new vessels are composed of vascular cells derived from two sources: vascular cells derived from adjacent normal vasculature and circulating vascular precursor cells derived from the bone marrow (BM).<sup>5-10</sup> In previous studies using bone marrow transplantation (BMT), we have shown that BM-derived endothelial and perivascular mesenchymal cells are present within the experimental CNV lesion and contribute to up to 40% of its cellular composition.<sup>11</sup> Similar results have been demonstrated in animal models of vascular injury, including retinal neovascularization, tumor neovascularization, and hind limb ischemia.<sup>12-14</sup> Bone marrow-derived precursor cells may be a source of cells that promote vascular repair in

ischemic tissue.<sup>15-18</sup> On the other hand, these cells may contribute to vascular injury. Cornacchia et al.<sup>19</sup> demonstrated that BMT from diabetic mice transfers renal glomerulosclerosis to nondiabetic recipients, and that diabetes-altered mesangial precursor cells from the BM were the causative cell type.<sup>19</sup>

In this study, we examined the role of BM-derived vascular precursor cells in the age-related regulation of NVR in experimental laser-induced CNV. We hypothesized that precursor cells derived from aged BM and transplanted into young recipients would transfer the severe NVR lesion phenotype observed in older animals. Our results showed that BM from aged mice indeed transferred susceptibility to NVR to young mice, and that the more severe lesions appeared to contain a greater proportion of circulating perivascular mesenchymal precursor cell derivatives, including both vascular smooth muscle cells and myofibroblasts, but not an increase in BM-derived endothelial cells.

## MATERIALS AND METHODS

### Animals

All animal experiments adhered to the ARVO Statement for the Use of Animals in Ophthalmic and Vision Research following institutionally approved protocols. Young (Y: 2-4 months) and old (O: 16-18 months) female wild-type C57BL/6J mice were purchased from the National Institute of Aging (NIA, Bethesda, MD) and served as "recipient" mice for BMT. The NIA aging breeding colonies were rederived from stocks obtained from The Jackson Laboratory (Bar Harbor, ME) in 2005, and do not carry the *Crb1*<sup>rd8</sup> mutation. The absence of the mutation was confirmed by PCR. Similarly, "donor" BM-derived whole or purified CD34+ cells were isolated from young and old female C57BL/6J transgenic mice expressing green fluorescent protein (GFP; The Jackson Laboratory).

### Murine Bone Marrow Transplantation

Bone marrow transplantation was performed as described previously.<sup>10</sup> Briefly, BM was extracted from either wild-type or GFP young and old donor mice ( $n = 10$  per cohort) by flushing RPMI-1640 medium in the diaphyseal channel of both tibias and femurs. Basement membrane was homogenized and filtered; and isolated unpurified BM cells, devoid of red blood cells, were transplanted into the retro-orbital sinus of lethally irradiated (950 cGy) young or old recipient mice ( $n = 8$  for each group). Blood components were allowed to reconstitute for 1 month before induction of experimental CNV. Chimerism was routinely greater than 90%. In a preliminary study, the heads of mice were shielded by a lead chamber during irradiation.

### Enrichment of Lineage-Negative Cells From Murine Bone Marrow

Whole BM cells were depleted of mature lineage-positive hematopoietic cells and enriched of precursor cells (Lineage Cell Depletion Kit; Miltenyi Biotec, Auburn, CA). Briefly, BM cells obtained from young ( $n = 10$ ) or old ( $n = 10$ ) donor mice were filtered through a 40- $\mu$ m cell strainer (BD Falcon, Franklin Lakes, NJ). A single-cell suspension of  $10^7$  cells was labeled with 20  $\mu$ L anti-Biotin microBeads (Miltenyi Biotec) and subjected to magnetic column separation using the autoMACS separator (Miltenyi Biotec, Auburn, CA). The enriched unlabeled lineage-negative cell fraction was eluted and collected for further manipulation.

### Adoptive Transfer of CD34+ Cells and Splenic Macrophages

CD34+ cells were enriched by incubating  $10^7$  whole BM cells, isolated as detailed above ( $n = 20$  young or old GFP mice) and devoid of red blood cells, with rat anti-mouse CD34+ conjugated with phycoerythrin (PE; BD Biosciences, Pharmingen, San Diego, CA) for 30 minutes at 4°C. Cells were then labeled with 20  $\mu$ L MACS anti-PE microBeads (Miltenyi Biotec) and subjected to magnetic column separation for positive isolation. CD34+ cells were 49% of total collected as determined by flow cytometry. For splenic macrophage isolation, spleens were harvested aseptically ( $n = 20$  young or old GFP mice), cut into small pieces, mashed with a spatula, and filtered to single-cell suspension. Splenocytes were subjected to a similar enrichment protocol, described above, using rat anti-mouse F4/80+ conjugated to PE (Abcam, Cambridge, MA). In both cases, cells were counted, and  $10^5$  CD34+ or F4/80+ cells were given intravenously to each recipient mouse ( $n = 8$  per group) immediately after the CNV laser procedure.

### Western Blot Analysis

Whole cell protein extracts (M-PER; Pierce Thermo Scientific, Rockford, IL) of unpurified BM or lineage-negative precursor cells were denatured in NuPAGE LDS sample buffer (Invitrogen Life Technologies, Grand Island, NY) under reducing conditions, separated on 4% to 12% gradient Bis-Tris gels, and transferred to nitrocellulose membranes. Primary antibodies and dilutions used were smooth muscle 22 (SM22, 1:1000; Abcam), von Willebrand factor (vWF, 1:200; Santa Cruz Biotechnologies, Santa Cruz, CA), and CD31 (1:200; Abcam). Secondary antibodies used were horseradish-peroxidase-conjugated donkey anti-mouse and donkey anti-rabbit (1:10,000 and 1:5000, respectively; Jackson ImmunoResearch, West Grove, PA). Immunoreactive bands were visualized by chemiluminescence (ECL Plus; GE HealthCare, Piscataway, NJ). All lanes were loaded with 15  $\mu$ g cell lysate. Relative differences between SM22 and CD31 or vWF expression for each condition were expressed as the ratio of densitometry between the two markers for each lane.

### Laser-Induced CNV Model, Fluorescein Angiography, and Choroidal Flat Mount Morphometric Analysis

One month after BMT or immediately after adoptive transfer, experimental CNV was induced according to published procedures.<sup>4</sup> At 4 weeks postlaser, all analyses were performed. Fluorescein angiography (FA) was performed in a subset of animals using a modified approach to a previously described technique.<sup>4</sup> Briefly, sodium fluorescein 10% (0.1 mL 100 mg/mL; Akorn, Decatur, IL) was injected intraperitoneally into anesthetized mice. The angiograms were recorded using a Spectralis scanning laser ophthalmoscope camera (Heidelberg Engineering, Vista, CA) using the FA setting. Photographs were obtained at approximately 1 and 4 minutes after dye injection. In some mice, in vivo perfusion with fluorescein isothiocyanate (FITC)-dextran was used to determine vascular area (Sigma-Aldrich, St. Louis, MO). All mice were then perfused intracardially with 4% paraformaldehyde (PFA) for 10 minutes and euthanized; eyes were removed for histopathological analysis (left eye) and choroidal flat mount analysis (right eye). The vascular surface area of CNV lesions in flat mounts was determined by evaluating the FITC-dextran-positive area. Cell density analysis of flat mounts was performed using propidium iodide (PI; Sigma-Aldrich) fluorescence as previous-

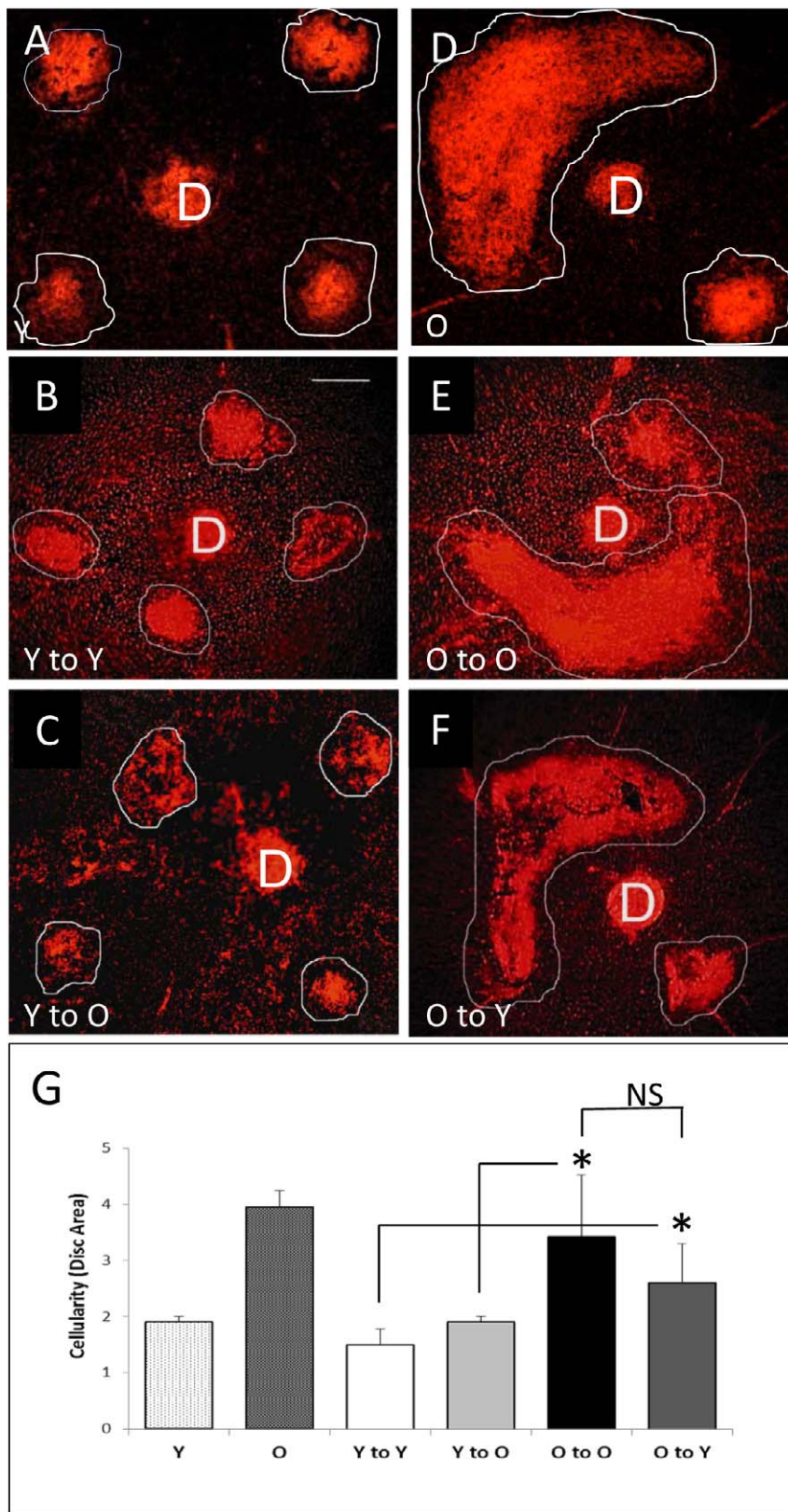


**FIGURE 1.** Quantitative analysis of cellular density in experimental CNV lesions developed in mice after BMT. Flat mounts were prepared from the posterior pole of recipient mice eyes and stained with propidium iodide. Small lesions developed in young unmanipulated mice (A) and also when young BM was transplanted into either young (B, Y-to-Y) or old mice (C, Y-to-O). In contrast, old unmanipulated mice (D) and the old-to-old group (E) developed large neovascular lesions with connections between adjacent lesions. Additionally, young recipients receiving old BM (F, O-to-Y) developed intermediate-size lesions, often with adjacent lesions becoming interconnected. (G) Quantitative analysis of the surface area of CNV lesions in each group. Significant differences were observed (*asterisks*) when old BM was transplanted in both young and old recipients in comparison with transplantation of young BM (*t*-test:  $P < 0.001$ ). D, optic disc. *White line* encircles CNV lesions. Magnification:  $\times 50$ ; *scale bar*: 200  $\mu\text{m}$ .

ly described.<sup>4</sup> Vascular morphology visualization was performed by incubating flat mounts overnight in either biotinylated lectin (BS-1, 1:1000; Sigma-Aldrich) or TRITC-lectin (1:100; Sigma-Aldrich). For area calculations, the lesion area in pixels was normalized by dividing the lesion area by the mean value of optic disc area (mean value of 10 independent eyes). A CNV was defined as present if the surface area of an individual lesion was more than 0.50 disc areas (the diameter of the laser burn).<sup>4</sup> The results are presented as relative disc areas.

### Histology and Immunohistochemistry

Eyes were postfixed for 1 hour in 4% PFA, cryoprotected, optimal cutting temperature (OCT) embedded, and snap frozen in liquid nitrogen. Serial sections (14  $\mu$ m) were either stained with hematoxylin-eosin for morphological evaluation or incubated overnight with the following antibodies: anti-GFP-Alexa 488 (1:1000; Molecular Probes—Life Technologies, Grand Island, NY), anti-F4/80 (1:500; AbD Serotec, Raleigh, NC), anti-alpha smooth muscle actin (SMA) conjugated to Cy3 (1:20,000; Sigma-Aldrich), anti-CD31 (PECAM-1, 1:500; Santa Cruz Biotechnology), or anti-collagen IV (1:400; Abcam). Immunostaining other than for GFP and SMA was visualized using Alexa 568-conjugated secondary antibodies (1:500; Molecular Probes—Life Technologies). Cell nuclei were stained with 4',6'-diamino-2-phenylindole (DAPI; Molecular Probes—Life Technologies). Slides were mounted with aqueous mounting medium (Crystal Mount; Biomedica, Foster City, CA) and coverslipped.

### Data Analysis

Serial cross sections of eyes containing CNV lesions were examined for the presence of GFP-labeled cells and expression of different cell markers using a fluorescent microscope (Axiophot Photomicroscope; Carl Zeiss Microscopy, Thornwood, NY) and a four-channel laser scanning confocal microscope (LSM 510; Carl Zeiss Microscopy). Images were digitally acquired (Axiovision or LSM Image Browser version 3.2; Carl Zeiss Microscopy) and recompiled (Photoshop 6.0; Adobe, San Jose, CA). For confocal imaging, thin optical sections (1  $\mu$ m) were examined to ensure that overlapping fluorescence was due to colocalization. Images shown are representative. The percentage of macrophages or endothelial or perivascular cells per lesion was calculated as the number of positive cells divided by DAPI-positive cells  $\times$  100. Cell numbers for each eye were calculated as the average from at least three sections from separate CNV lesions per eye. Morphometric data resulting from flat mount and histological samples for different lesions in each eye were averaged ( $n = 8$ ) to provide one value per eye. Data are presented as the mean  $\pm$  SEM. Statistical tests (*t*-test, ANOVA) were used to compare treatments and groups using Prism 4.0 (GraphPad Software, La Jolla, CA).

## RESULTS

### Characteristics of CNV Lesions After BMT From Young or Old Donors

We have previously shown that CNV lesions that develop in aged mice are approximately 2- to 3-fold larger than in young mice, manifesting larger-caliber vessels and more fibrosis.<sup>4</sup> In the present study, we sought to evaluate age-dependent regulation of CNV severity by BM resident cells by performing BMT. Six total groups were assessed. Two groups were normal

controls, representing young and old mice, which did not receive irradiation and BMT. The other four groups consisted of 8 recipient and 10 donor wild-type mice each. Two groups represented controls of young and old recipient mice receiving whole BM from age-matched animals (young-to-young [Y-to-Y] and old-to-old [O-to-O]). Two experimental groups consisted of mice engrafted with whole BM isolated from old donors into young animals (old-to-young [O-to-Y]) and vice versa (young-to-old [Y-to-O]).

We used choroidal flat mount analysis of cellular density to determine CNV size. As shown previously, normal young mice (Fig. 1A) demonstrated small lesions while normal aged mice developed large lesions (Fig. 1D). The group of young mice receiving BMT from young donors (Y-to-Y) developed small CNV lesions (Fig. 1B,  $1.49 \pm 0.29$  disc areas [DA]), similar in size to those observed in unmanipulated young mice. Further, old mice receiving BMT from old donors (O-to-O) developed large CNV lesions (Fig. 1E,  $3.42 \pm 1.1$  DA), comparable to those in unmanipulated old mice. Thus, irradiation and BMT process did not specifically alter the lesion size from the expected outcomes in unmanipulated mice. In contrast, when aged mice received BM from young mice, they developed small lesions similar to those in young mice (Fig. 1C,  $1.9 \pm 0.1$  DA). Conversely, young mice that received aged (O-to-Y) BMT developed intermediate-size lesions (Fig. 1F,  $2.60 \pm 0.69$  DA). Comparative analysis of differences in CNV area of the six groups is shown in Figure 1G. Statistically significant differences were observed between mice receiving BMT of Y-to-Y versus O-to-Y and Y-to-O versus O-to-O. However, mice receiving O-to-O versus O-to-Y and Y-to-Y versus Y-to-O were not different. In summary, BMT transferred susceptibility to disease severity in laser-induced CNV according to the age of the BM donor. That is, old BM transferred susceptibility to the development of intermediate-to-large lesions into young mice, and young BM prevented old recipient mice from developing large lesions.

We evaluated the vascularity pattern of laser CNV among different groups using FA and analysis of CNV vascular lesion flat mounts. Representative FA images taken at early ( $\sim$ 1 minute, Figs. 2A, 2D, 2G) and late ( $\sim$ 4 minutes, Figs. 2B, 2E, 2H) time points demonstrate relative lesion sizes and associated leakage activity across groups. Young mice demonstrated small well-circumscribed lesions with minimal late leakage (Figs. 2A, 2B), while old mice demonstrated large, often confluent lesions, with active late leakage (Figs. 2D, 2E). Lesions in young mice receiving old marrow (O-to-Y) demonstrated intermediate-size lesions, but also with active late leakage (Figs. 2G, 2H).

TRITC-lectin-labeled flat mount images representing specific lesions on the FA demonstrated distinct differences in vascular morphology. Young mice demonstrated small lesions with small-caliber vascular networks (presumed capillaries), minimal discernible arterioles, and well-demarcated margins (Fig. 2C). In contrast, old mice (Fig. 2F) demonstrated large lesions composed of some small capillaries, many large-diameter branching arterioles (Fig. 2F, arrow), and extensions of large-diameter vascular loops at the lesion margins (Fig. 2F, arrowhead). O-to-Y mice had intermediate-size lesions (Fig. 2I) but with vascular morphology similar to that of lesions in old mice: some capillaries and marginal vascular loops (arrowhead) and many large-caliber branching arterioles (arrows). The presence of large-caliber arterioles and marginal vascular loops is consistent with NVR.

Finally, measurement of vascular surface area across transplant groups by FITC-dextran perfusion was consistent with the FA and cellular flat mount results for lesion size. Bone marrow transplantation of Y-to-Y resulted in small vascular area; BMT of O-to-O resulted in large vascular area; and BMT of

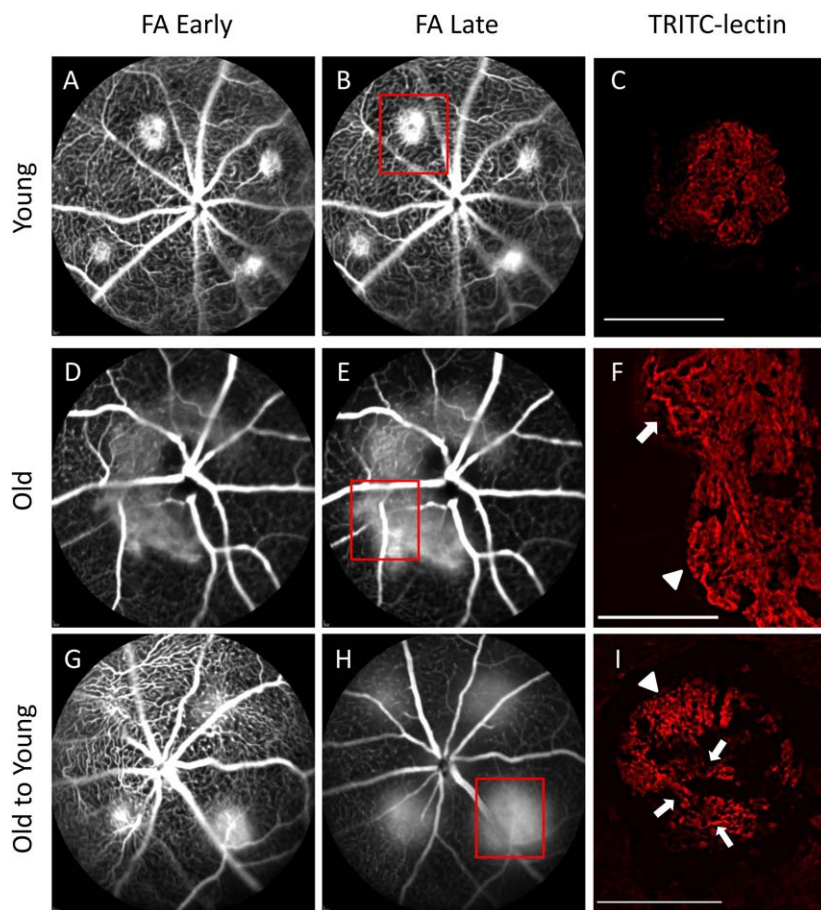


**FIGURE 2.** Vascular morphology in experimental CNV lesions by fluorescein angiography and lectin-stained flat mount. Early (~1 minute) and late (~4 minutes) FA photographs were obtained to characterize lesion size and leakage activity of experimental CNV. Lectin-stained vascular flat mounts were obtained to characterize differences in vascular morphology (magnification:  $\times 100$ ; scale bars: 100  $\mu\text{m}$ ). Young mice demonstrated small lesions, well-demarcated borders, and mild fluorescein leakage (A, B). Lectin-stained flat mount analysis of one of these lesions (corresponding to red box [B]) demonstrated well-defined, small-diameter capillary networks with minimal discernible large-caliber arterioles (C). FA from old mice demonstrated large, confluent CNV with very active fluorescein leakage (D, E). Lectin-stained flat mount from one of these CNV lesions (corresponding to red box [E]) revealed many large branching arterioles (arrow) and vascular loops at the lesion margins (arrowhead) (F). Lesions from young mice transplanted with old marrow (O-to-Y) demonstrated intermediate size but very active fluorescein leakage (G, H). Lectin-stained flat mount from one lesion (corresponding to red box [H]) revealed morphology similar to that of lesions in old eyes, including some capillaries and marginal vascular loops (arrowhead), and many large-caliber branching arterioles (arrows) (I).

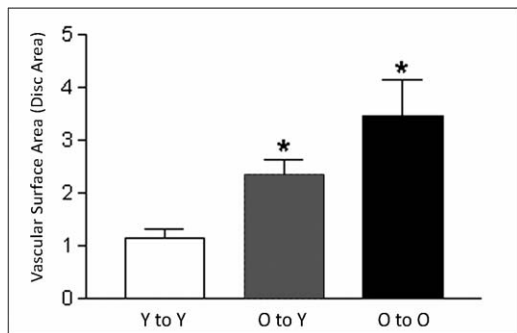


**FIGURE 3.** Quantitative analysis of vascular surface area in experimental CNV lesions after BMT. Quantitative analysis of the vascular surface area of CNV lesions (FITC-dextran perfusion) of each group showed significant differences (asterisks) between the young-to-young compared to the old-to-young and the old-to-old groups (*t*-test:  $P < 0.003$ ) and among all three groups (ANOVA:  $P < 0.0017$ ). The differences between old-to-young and old-to-old were not statistically significant.

O-to-Y transferred intermediate-sized vascular lesions into the young recipients. These were significantly larger than lesions in the Y-to-Y group (Fig. 3).

We used histopathology to compare cross-sectional morphology of experimental CNV after BMT. Sections from the Y-to-Y group revealed small lesions (Fig. 4A), which were comparable to those previously observed in unmanipulated young mice.<sup>4</sup> In contrast, sections from the O-to-Y group revealed large, thick CNV lesions (Fig. 4B). Comparison of the mean cross-sectional area between the Y-to-Y and the O-to-Y group showed a 62% size increase (Fig. 4C,  $70.6 \pm 11.7$  vs.  $114.7 \pm 20.6 \times 1000 \text{ pixels}^2$ ). In a pilot experiment, the head of recipient mice was shielded from irradiation without apparent change in the morphology or outcome (data not shown). Thus, no evidence of radiation retinopathy or other potential changes from the irradiation required for BMT were apparent.

Aged BMT was found to increase the frequency of large lesions. Using 1.9 disc area cutoff (representing the 95% confidence interval for lesion size in unmanipulated young mice), only 14% of the total number of lesions in Y-to-Y

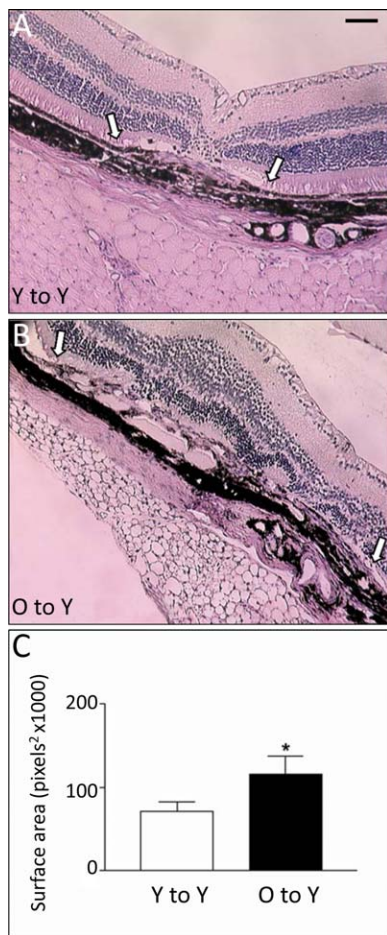


**FIGURE 4.** Histopathology sections of experimental CNV after young or old BMT into young recipient mice. Sections were stained with hematoxylin and eosin. CNV lesions were significantly less severe in young mice that received young BM ([A], Y-to-Y) when compared with young mice transplanted with old BM ([B], O-to-Y). *White arrowheads* show the margins of the CNV membranes. (C) A significant difference in lesion size was observed between the two transplanted groups when the mean cross-sectional area was quantitatively analyzed. Magnification:  $\times 100$ ; scale bar: 100  $\mu\text{m}$ .

exceeded this size. In contrast, the frequency of intermediate-to-large lesions in O-to-O was 85%. In young mice receiving old BM, the frequency of intermediate-to-large lesions was 69%. Taken together, these results indicate that the age of the BM, and not the age of the choroid, Bruch's membrane, and outer retina, is the primary determinant of CNV severity. This finding suggests that cellular components present in aged BM regulate the degree of fibrosis, size, and vascular maturation.

#### Contribution of Different Cell Subtypes to CNV Lesions in Mice Receiving Young or Old BM

To characterize the identity of cells within each lesion, experimental-laser CNV lesions from young recipients receiving either young or old BM were analyzed with specific cell markers for macrophages (F4/80), endothelial cells (CD31), or perivascular mesenchymal cells (SMA). The proportion of F4/80+ blood-derived macrophages was identical in the two groups (23% in Y-to-Y and 24% in O-to-Y, data not shown). Also, in spite of the substantial difference in lesion size, the proportion of endothelial cells present was not significantly

different between young mice receiving young or old marrow (Fig. 5A,  $36.3 \pm 0.04\%$  vs.  $40.5 \pm 0.05\%$ , respectively).

We previously demonstrated that CNV lesions in non-transplanted old mice were not only larger but also more fibrotic and demonstrated more SMA+ cells, presumably representing perivascular mesenchymal precursor-derived cell types such as pericytes, vascular smooth muscle cells, or myofibroblasts.<sup>4</sup> Similar findings were observed in the O-to-Y group, in which the frequency of SMA-expressing cells was significantly greater than in the Y-to-Y group ( $34.2 \pm 0.04\%$  O-to-Y versus  $18.7 \pm 0.01\%$  Y-to-Y, Fig. 5B). Conversely, the degree of fibrosis and proportion of SMA+ cells in the Y-to-O group was not statistically different from values in the Y-to-Y group (Fig. 5C), indicating that young marrow conveys the young perivascular mesenchymal phenotype into old recipients.

Immunohistochemistry was performed to detect collagen type IV levels in order to demonstrate qualitative changes in extracellular matrix deposition, another well-known sign of fibrosis. As expected, small lesions from unmanipulated young mice (Fig. 6A) showed less collagen IV immunoreactivity than large lesions in aged mice (Fig. 6B). Old mice receiving BMT from young donors demonstrated collagen deposition similar to that in the unmanipulated young mice (Fig. 6C).

#### Contribution of Resident Versus Recruited Bone Marrow Cell Subtypes to CNV Lesions After BMT

In BMT experiments using young GFP donor cells, we have observed that up to 40% of the endothelial and perivascular mesenchymal cell types within CNV lesions are BM derived.<sup>10,20</sup> Using young or old GFP-labeled BM, we differentiated between the relative proportion of resident-derived and recruited donor-derived endothelial and perivascular mesenchymal cell subsets. No difference was observed between young mice engrafted with young or old BM in terms of proportion of total CD31, resident-derived (GFP-/CD31+), or recruited marrow-derived (GFP+/CD31+) endothelial cells (Fig. 7C, top). In terms of SMA+ perivascular mesenchymal cells, both groups of mice (Y-to-Y and O-to-Y) demonstrated high frequency of resident SMA-expressing cells (red, arrowheads) and GFP-labeled BM-derived cells; many more double-positive cells (yellow, arrows), representing BM-derived SMA/GFP-expressing cells, were observed in cross sections from mice receiving old marrow (Figs. 7A, 7B). Quantitative assessment (Fig. 7C, bottom) revealed that the proportion of total SMA+ population was significantly greater in O-to-Y than in Y-to-Y, similar to data in Figure 5. Although the specific resident-derived subset of SMA+ perivascular mesenchymal cells was greater in O-to-Y than in Y-to-Y, the differences in proportion were less than observed for the total SMA+ group. However, recruited, marrow-derived SMA+ cells demonstrated a greater increase (almost 2.5-fold) in O-to-Y than in Y-to-Y. We conclude that the greatest difference in cellular subsets was the significantly increased proportion of BM-derived SMA+ perivascular mesenchymal cells in mice with severe CNV after receiving aged BMT. No subset of endothelial cells showed any proportional increase in mice receiving old BM with severe CNV.

#### Engraftment of CD34+ and F4/80+ Cells Following Adoptive Transfer

We have previously shown that macrophage infiltration contributes to increased CNV severity.<sup>21</sup> To further differentiate the relative contribution of BM vascular cells from macrophages, and to rule out possible artifacts induced by the total body irradiation required prior to BMT, adoptive

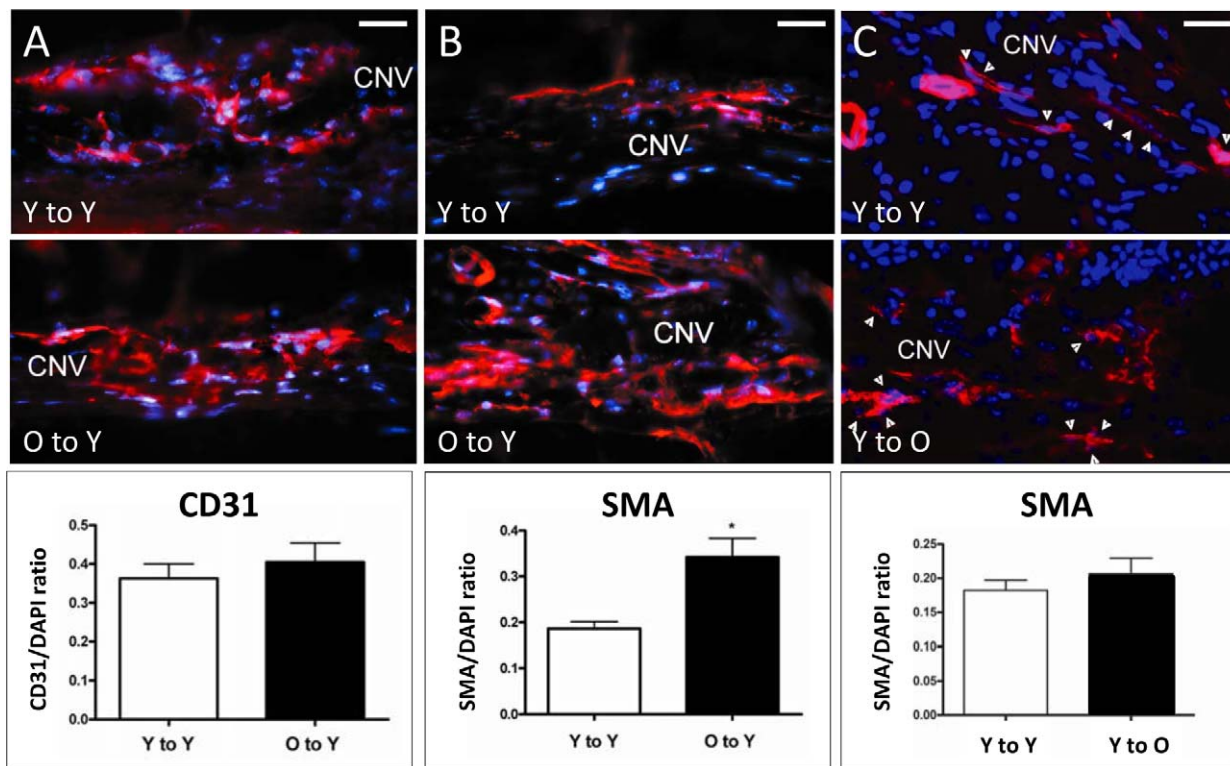


**FIGURE 5.** Immunofluorescence detection of endothelial and perivascular mesenchymal cells present in CNV lesions after BMT. Endothelial cells were stained with CD31 (*left*) and perivascular mesenchymal cells with SMA (*center and right*). In spite of the difference in lesion size, the frequency of endothelial cells (**A**) was not significantly different between the young-to-young ( $36.3 \pm 0.04\%$ ) and the old-to-young group ( $40.5 \pm 0.05\%$ ). In contrast, a significant increase (*asterisk*) in the frequency of SMA-expressing cells (**B**) was observed when the old-to-young group ( $34.2 \pm 0.04\%$ ) was compared to the young-to-young group ( $18.7 \pm 0.01\%$ , *t*-test:  $P < 0.002$ ). (**C**) No significant increase in the frequency of SMA-expressing cells (*arrowheads*) was observed between the young-to-young ( $18.22 \pm 0.01\%$ ) and the young-to-old group ( $20.7 \pm 0.02\%$ , *t*-test:  $P = 0.360$ ). Magnification:  $\times 400$ ; scale bars: 100  $\mu\text{m}$ ; CD31 (*left*) or SMA (*center and right*), red; DAPI, blue.

transfer experiments were performed. Although no definitive marker specifically identifies the BM perivascular mesenchymal precursor population, they are thought to express CD34 (also expressed on some monocyte precursors, endothelial precursors, and other cell types).<sup>22</sup> Unmanipulated mice received intravenous infusion of CD34+ cells purified from BM or F4/80 splenic macrophages, purified from young or old GFP+ mice. Laser treatment to induce experimental CNV was done on the same day as cellular infusion or 1 week prior to infusion.

As shown in Figures 8A and 8B, young mice receiving CD34+ cells from old marrow developed significantly larger lesions than those receiving young CD34+ cells (Fig. 8C,  $2.8 \pm$

$0.4$  vs.  $1.5 \pm 0.1$  DA, *t*-test:  $P < 0.0115$ ). Immunohistochemistry of CNV lesions from mice receiving old CD34+ cells showed incorporation of CD34+/GFP+ marrow cells into the lesions (Fig. 8D). Interestingly, no significant difference in lesion size was observed in young mice receiving either young or old F4/80+ macrophages (Fig. 8E). The timing of the adoptive transfer during the course of CNV development was important in terms of transferring the more severe phenotype. When cells were transferred 7 days after CNV induction rather than on the same day, adoptive transfer of CD34+ cells from old marrow did not produce the expected increase in severity (Fig. 8E). These results suggest that cells resident within the

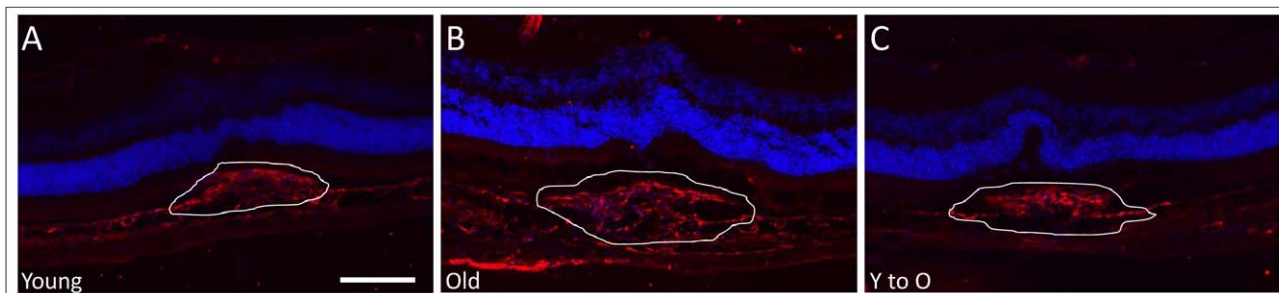


**FIGURE 6.** Levels of collagen type IV deposition present in CNV lesions. Cryosections with representative CNV lesions were stained with an antibody to collagen type IV to determine extent of fibrosis in the different groups. The amount of collagen IV deposition was greater in CNV lesions of old (**B**) compared to those of young (**A**) unmanipulated mice. In contrast, a decrease in collagen deposition was observed in CNV lesions in young-to-old mice (**C**) when compared to old unmanipulated mice. *White lines* outline neovascular lesions. Magnification:  $\times 200$ ; scale bar: 100  $\mu\text{m}$ . Collagen type IV (red), DAPI (blue).

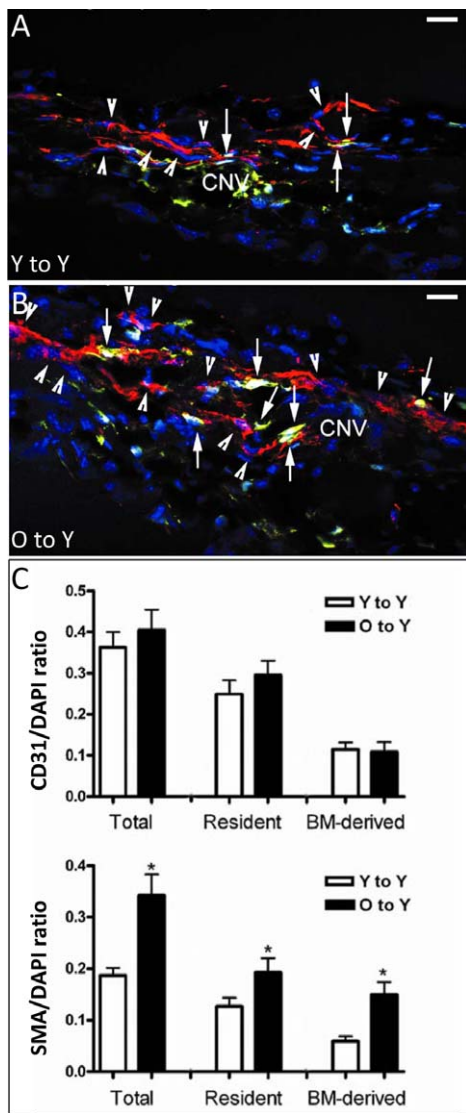


**FIGURE 7.** Immunofluorescence detection of resident or recruited BM-derived SMA-expressing perivascular mesenchymal cells in CNV lesions after BMT. Young mice received young (A) or old (B) GFP BM, followed by laser-induced CNV. Although both groups demonstrated high frequency of resident SMA-expressing cells (red, arrowheads) and GFP-labeled BM-derived cells, many more double-positive cells (yellow, arrows), representing BM-derived SMA/GFP-expressing cells, were observed in cross sections from mice receiving old marrow. Quantification of the frequency of total, resident, and BM-derived CD31 endothelial cells ([C], top) showed no difference in resident or BM-derived CD31-expressing endothelial cells between mice receiving young or old marrow. In contrast, significant differences (asterisks) were observed in the frequency of both resident and BM-derived SMA-expressing cells in CNV of mice receiving marrow from young versus old donors ([C], bottom). In particular, mice receiving old marrow had a 2.5-fold increase in marrow-derived SMA-expressing perivascular mesenchymal cells, contributing to nearly half of all SMA-expressing cells in the CNV. SMA, red; GFP, green; colocalization of GFP and SMA, yellow; DAPI, blue. Magnification:  $\times 400$ ; scale bars: 20  $\mu\text{m}$ .

CD34+ cell subset of the BM are crucial in the development of NVR. Importantly, the causative cells must be present early during lesion development in order to transfer the more severe phenotype. Finally, these findings support the conclusion that irradiation-induced artifact did not account for the observed increased severity after BMT.

## Expression Levels of Perivascular and Endothelial Markers in BM From Young and Old Mice

One possible explanation for the previous results is that old BM contains a greater number or proportion of mesenchymal-derived perivascular precursor cells. We sought to determine if BM from old and young mice contained different relative proportions of endothelial precursors and perivascular mesenchymal precursors. We evaluated the relative expression of endothelial and perivascular mesenchymal markers in whole BM, freshly isolated lineage-negative cells, and CD34+ isolated cells (Fig. 9A). Western blot analysis revealed a higher expression of the mesenchymal marker SM22 in old compared to young whole BM. In contrast, BM cells isolated from young and aged mice showed similar expression of the endothelial-specific marker vWF.

Whole marrow contains “mature” nonprecursor mesenchymal populations that also express SM22 (i.e., fibroblasts). To confirm that an authentic population of mesenchymal-derived perivascular precursor cells, and not merely contaminating fibroblasts, was present in the marrow, we evaluated SM22 expression in subpopulations enriched for precursors but excluding fibroblasts. As shown in Figure 9B, enriched CD34+ cells also expressed SM22, excluding fibroblast contamination. However, CD34+ cells isolated from old marrow demonstrated higher relative expression of SM22 as compared to young CD34+ cells. In contrast, comparable expression of the endothelial-specific marker CD31 was observed between young and old. These results suggest that the ratio of perivascular mesenchymal precursor cells to endothelial precursor cells increases with age, or conversely, the number of endothelial precursor cells decreases with age (Fig. 9B). Taken together with data from Figures 7 and 8, this observation adds support for the hypothesis that BM-derived perivascular derivatives within CNV may originate from the CD34+ subset within the BM, and that increased number or proportion of CD34+ mesenchymal-derived perivascular precursor cells in older mice might be important in the development of NVR.

## DISCUSSION

Two main conclusions about laser-induced CNV can be drawn from these data. First, this study confirms our prior work showing that aging is associated with NVR, defined as increase in size, leakage activity, arteriolar-predominant vascular morphology, perivascular fibrosis, and proportion of SMA+ perivascular mesenchymal cells relative to endothelial cells when compared to values in young mice with small, capillary-like lesions.<sup>4,10,11</sup> Second, susceptibility to NVR is conveyed by the chronologic age of cells within the BM, and not by the chronologic age of the retina or choroid.

These data also suggest that perivascular mesenchymal precursor cells with the aged marrow are important for the development of NVR in CNV and specifically raise the possibility that circulating perivascular mesenchymal precursor cells may contribute to NVR directly by differentiating into vascular smooth muscle cells and/or myofibroblasts,<sup>23</sup> a previously undescribed phenomenon that will require further study. Choroidal neovascularization with NVR demonstrated almost 2.5-fold more marrow-derived perivascular mesenchymal SMA+ cells than in small, capillary CNV. However, we cannot exclude endothelial to myofibroblast transition.<sup>24</sup>

How does aged bone marrow regulate NVR? One possibility may be due to an increased frequency of marrow precursors with age. However, since BM contains macrophages as well as perivascular mesenchymal precursors, we cannot exclude the impact of age on monocytes. In fact, it is likely that both



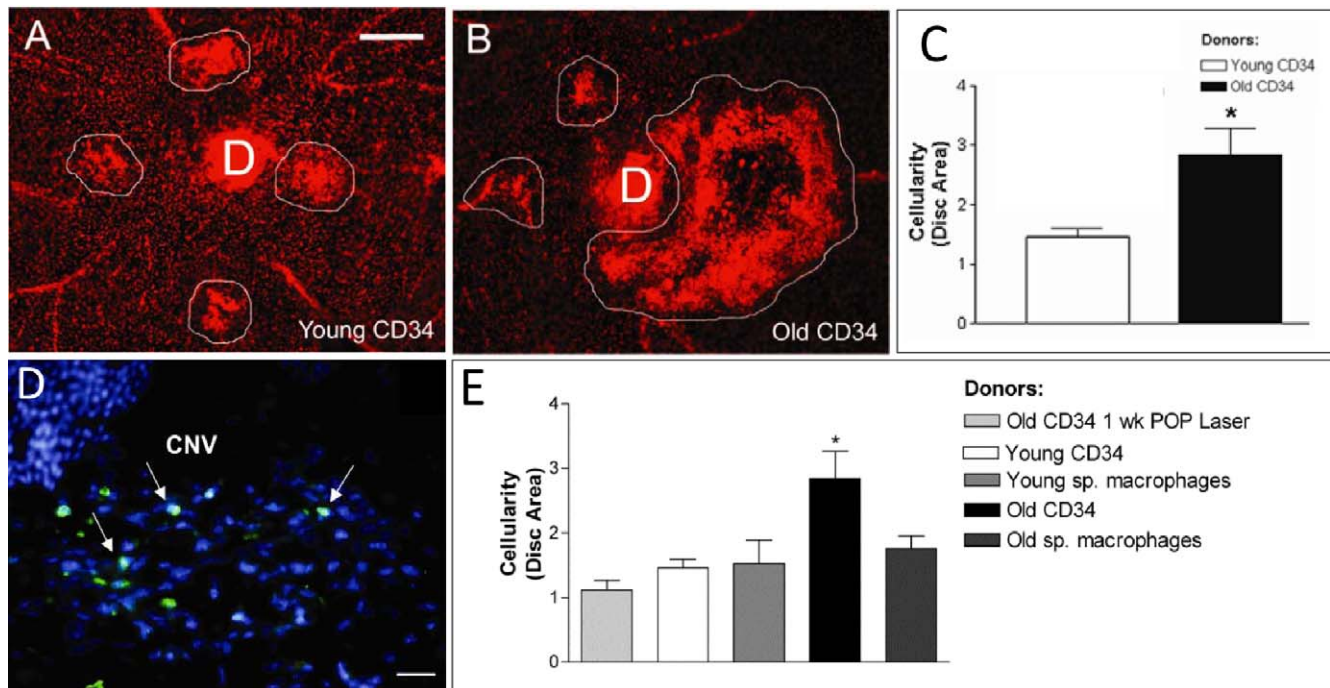


**FIGURE 8.** Analysis of CNV lesions in young animals receiving adoptive transfer of CD34<sup>+</sup>-GFP-labeled cells. CD34<sup>+</sup> precursor cells obtained from young or old donors were adoptively transferred to young recipient mice at the time of laser-induced CNV (without prior irradiation or BMT). Flat mounts were prepared and stained with PI. (A) Mice receiving adoptive transfer of CD34<sup>+</sup> cells isolated from a young donor display typical small CNVs. (B) In contrast, animals receiving adoptive transfer of CD34<sup>+</sup> cells from old donors developed large CNVs. D, optic disc; *white lines* encircle CNV lesions. Magnification:  $\times 50$ ; *scale bar*: 200  $\mu$ m. (C) Quantitative analysis of surface area showed a significant size increase (*asterisk*) in animals engrafted with CD34<sup>+</sup> cells from old donors as compared with young donors. (D) Immunohistochemistry of mouse eye cross sections with CNV lesion showed recruitment and engraftment of adoptively transferred GFP<sup>+</sup> cells (*arrows*) within 3 days after CNV induction. GFP, *green*; DAPI, *blue*. Magnification:  $\times 400$ ; *scale bar*: 20  $\mu$ m. (E) Quantitative analysis of cellular density after adoptive transfer of young or old CD34<sup>+</sup> cells versus young or old macrophages (F4/80). Mice receiving old CD34<sup>+</sup> cells developed CNV lesions that are approximately double in size (*asterisk*) when compared to those in the other groups. Adoptive transfer of young or old F4/80<sup>+</sup> splenic macrophages failed to induce any increase in severity, similarly to adoptive transfer of CD34<sup>+</sup> cells from old marrow transferred 7 days after CNV induction.

macrophages and perivascular mesenchymal precursors are necessary for NVR. Apte and others have demonstrated the important role of aged macrophages in regulating CNV severity.<sup>25</sup> Circulating BM-derived perivascular mesenchymal precursor cells might be recruited into the lesion by factors including stromal cell-derived factor-1 (SDF-1),<sup>26</sup> platelet-derived growth factor-AB (PDGF-AB), insulin-like growth factor 1 (IGF-1),<sup>27</sup> and osteopontin.<sup>28</sup> A reasonable hypothesis is that macrophages may be a major source of the factors promoting the chemotaxis and differentiation of perivascular mesenchymal precursor cells.

Adoptive transfer experiments of CD34<sup>+</sup> cells in young mouse recipients in concert with SM22 expression data in whole BM and CD34<sup>+</sup> cells suggest that old CD34<sup>+</sup> perivascular precursors transfer age-related pathology by directly incorporating into the CNV lesion. Although adoptive transfer did not precisely mimic the biology of whole BM transplantation, our results argue against radiation-induced artifacts as an important mechanism in our observation.<sup>29</sup> In addition, the ability of adoptive transfer to recreate the lesion severity suggests that the contribution of precursors to the severe phenotype probably occurs early in the neovascular process. This result is evident not only from our current findings (i.e., old CD34<sup>+</sup> cells transferred late in the induction process of CNV lesions) but also since the adoptively transferred cells are likely to be cleared from the circulation within a few days after administration.<sup>29</sup>

Another potential difficulty in interpreting our results is that the laser-CNV model used in this study may not completely

recapitulate all the feature of human CNV lesions. Nevertheless, the morphology of human CNV is highly variable, and many examples do demonstrate extensive fibrosis and branching new vessels similar to this model.<sup>30</sup> Also, we have previously shown that vascular precursors contribute significantly in a model of CNV driven by VEGF overexpression.<sup>20</sup> Thus, we believe that our results can be extrapolated to human CNV in AMD in which the pathophysiology is more complex.

Another complexity in interpretation of our results is the variability in lesion size in O-to-Y mice as well as in old mice without radiation or BMT. Generally, within an experiment, there is less variability in lesion size in young mice with small lesions. Some of the variability in other groups is statistical (large lesions have greater potential ranges in size, creating more variation) as well as biological (unknown variations in environmental insults and exposures over a mouse lifetime that regulate the severe aging phenotype in the marrow). The observation that lesion size in O-to-Y mice was intermediate between young and old unmanipulated mice might also suggest that there are factors in addition to the BM that regulate lesion size. However, with all the data taken together, we believe that the consistent differences between young mice and O-to-Y mice observed across multiple CNV parameters (size, leakage, vascular morphology, perivascular fibrosis, and cellular composition) were not only statistically significant but also physiologically meaningful.

The clinical relevance of these findings is that circulating perivascular mesenchymal precursor cells may play a role in regulating the severity of human CNV. The concept that NVR

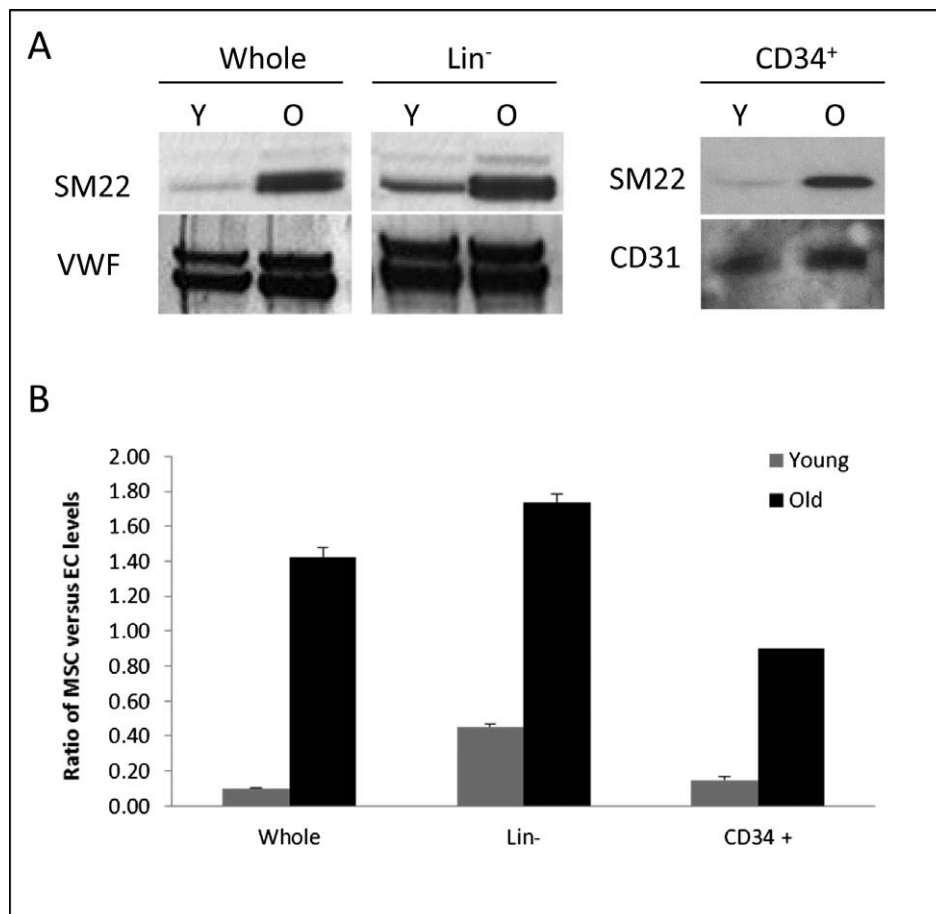


**FIGURE 9.** Western blot analysis of BM cells isolated from young and old mice. Cells were obtained either from whole BM (*left*) or a lineage-negative (*center*) or a CD34<sup>+</sup> subpopulation (*right*). Expression levels of endothelial (vWF or CD31) and mesenchymal (SM22) markers were analyzed via Western blotting (A). Ratio of SM22 levels versus endothelial markers (vWF or CD31) was quantified as internal loading control in each lane (B). Whole old BM showed a significantly higher expression of SM22 when compared to young BM, while vWF did not change significantly between the different age group. To exclude contamination from mature cell populations (i.e., fibroblasts), precursor-enriched populations (lineage negative or CD34<sup>+</sup> enriched) demonstrated similar pattern of increased SM22 expression in old compared to young mice compared to CD31. This result strongly suggests that the SM22<sup>+</sup> cells were mesenchymal precursor cells.

contributes to human neovascular AMD and has therapeutic implications is relatively new (Mettu PS, et al. *IOVS* 2012;53:ARVO E-Abstract 2654). Postmortem and surgically excised histopathological specimens of human CNV demonstrate that they are not simple endothelial lined tubes, but are morphologically complex fibrovascular lesions containing many different cells types with significant extracellular matrix and fibrosis.<sup>30</sup> In vivo imaging technologies reveal a diverse pattern of vascular maturation in human CNV ranging from capillary subtypes to arteriolarized vascular complexes with minimal capillary structure. Large lesions in patients tend to be more arteriolarized and fibrotic.<sup>31</sup> Recent clinical trial data documented that 50% to 80% of eyes with neovascular AMD demonstrate residual vascular leakage in spite of a year of anti-VEGF therapy,<sup>32</sup> indicating that neovascular AMD lesions demonstrate differential sensitivity to anti-VEGF therapy. We hypothesize that many of these resistant cases are caused by CNV with neovascular remodeling.

#### Acknowledgments

The authors thank Karen Wu for technical assistance with immunohistochemistry experiments.

Supported by National Institutes of Health Grant EY018880-01. The authors alone are responsible for the content and writing of the paper.

Disclosure: **D.G. Espinosa-Heidmann**, None; **G. Malek**, None; **P.S. Mettu**, None; **A. Caicedo**, None; **P. Saloupis**, None; **S. Gach**, None; **A.K. Dunnnon**, None; **P. Hu**, None; **M.-G. Spiga**, None; **S.W. Cousins**, None

#### References

- Jaffe GJ, Martin DF, Toth CA, et al. Macular morphology and visual acuity in the Comparison of Age-related Macular Degeneration Treatments Trials. *Ophthalmology*. 2013;120:1860-1870.
- Nunes SS, Greer KA, Stiening CM, et al. Implanted microvessels progress through distinct neovascularization phenotypes. *Microvasc Res*. 2010;79:10-20.
- Suner IJ, Espinosa-Heidmann DG, Marin-Castano ME, Hernandez EP, Pereira-Simon S, Cousins SW. Nicotine increases size and severity of experimental choroidal neovascularization. *Invest Ophthalmol Vis Sci*. 2004;45:311-317.
- Espinosa-Heidmann DG, Suner I, Hernandez EP, Frazier WD, Csaky KG, Cousins SW. Age as an independent risk factor for

- severity of experimental choroidal neovascularization. *Invest Ophthalmol Vis Sci.* 2002;43:1567-1573.
5. Folkman J. Angiogenesis in cancer, vascular, rheumatoid and other disease. *Nat Med.* 1995;1:27-31.
  6. Kalka C, Asahara T, Krone W, Isner JM. Angiogenesis and vasculogenesis. Therapeutic strategies for stimulation of postnatal neovascularization [in German]. *Herz.* 2000;25:611-622.
  7. Asahara T, Murohara T, Sullivan A, et al. Isolation of putative progenitor endothelial cells for angiogenesis. *Science.* 1997;275:964-967.
  8. Ozerdem U, Alitalo K, Salven P, Li A. Contribution of bone marrow-derived pericyte precursor cells to corneal vasculogenesis. *Invest Ophthalmol Vis Sci.* 2005;46:3502-3506.
  9. Kassmeyer S, Plendl J, Custodis P, Bahramsoltani M. New insights in vascular development: vasculogenesis and endothelial progenitor cells. *Anat Histol Embryol.* 2009;38:1-11.
  10. Espinosa-Heidmann DG, Caicedo A, Hernandez EP, Csaky KG, Cousins SW. Bone marrow-derived progenitor cells contribute to experimental choroidal neovascularization. *Invest Ophthalmol Vis Sci.* 2003;44:4914-4919.
  11. Espinosa-Heidmann DG, Reinoso MA, Pina Y, Csaky KG, Caicedo A, Cousins SW. Quantitative enumeration of vascular smooth muscle cells and endothelial cells derived from bone marrow precursors in experimental choroidal neovascularization. *Exp Eye Res.* 2005;80:369-378.
  12. Asahara T, Masuda H, Takahashi T, et al. Bone marrow origin of endothelial progenitor cells responsible for postnatal vasculogenesis in physiological and pathological neovascularization. *Circ Res.* 1999;85:221-228.
  13. Grant MB, May WS, Caballero S, et al. Adult hematopoietic stem cells provide functional hemangioblast activity during retinal neovascularization. *Nat Med.* 2002;8:607-612.
  14. Zhang ZG, Zhang L, Jiang Q, Chopp M. Bone marrow-derived endothelial progenitor cells participate in cerebral neovascularization after focal cerebral ischemia in the adult mouse. *Circ Res.* 2002;90:284-288.
  15. Hristov M, Erl W, Weber PC. Endothelial progenitor cells: mobilization, differentiation, and homing. *Arterioscler Thromb Vasc Biol.* 2003;23:1185-1189.
  16. Hristov M, Weber C. Endothelial progenitor cells: characterization, pathophysiology, and possible clinical relevance. *J Cell Mol Med.* 2004;8:498-508.
  17. Isner JM, Kalka C, Kawamoto A, Asahara T. Bone marrow as a source of endothelial cells for natural and iatrogenic vascular repair. *Ann N Y Acad Sci.* 2001;953:75-84.
  18. Alev C, Li M, Asahara T. Endothelial progenitor cells: a novel tool for the therapy of ischemic diseases. *Antioxid Redox Signal.* 2011;15:949-965.
  19. Cornacchia F, Fornoni A, Plati AR, et al. Glomerulosclerosis is transmitted by bone marrow-derived mesangial cell progenitors. *J Clin Invest.* 2001;108:1649-1656.
  20. Csaky KG, Baffi JZ, Byrnes GA, et al. Recruitment of marrow-derived endothelial cells to experimental choroidal neovascularization by local expression of vascular endothelial growth factor. *Exp Eye Res.* 2004;78:1107-1116.
  21. Caicedo A, Espinosa-Heidmann DG, Pina Y, Hernandez EP, Cousins SW. Blood-derived macrophages infiltrate the retina and activate Muller glial cells under experimental choroidal neovascularization. *Exp Eye Res.* 2005;81:38-47.
  22. Krause DS, Ito T, Fackler MJ, et al. Characterization of murine CD34, a marker for hematopoietic progenitor and stem cells. *Blood.* 1994;84:691-701.
  23. Anjos-Afonso F, Bonnet D. Prospective identification and isolation of murine bone marrow derived multipotent mesenchymal progenitor cells. *Best Pract Res Clin Haematol.* 2011;24:13-24.
  24. Piera-Velazquez S, Li Z, Jimenez SA. Role of endothelial-mesenchymal transition (EndoMT) in the pathogenesis of fibrotic disorders. *Am J Pathol.* 2011;179:1074-1080.
  25. Kelly J, Ali Khan A, Yin J, Ferguson TA, Apte RS. Senescence regulates macrophage activation and angiogenic fate at sites of tissue injury in mice. *J Clin Invest.* 2007;117:3421-3426.
  26. Kucia M, Ratajczak J, Reza R, Janowska-Wieczorek A, Ratajczak MZ. Tissue-specific muscle, neural and liver stem/progenitor cells reside in the bone marrow, respond to an SDF-1 gradient and are mobilized into peripheral blood during stress and tissue injury. *Blood Cells Mol Dis.* 2004;32:52-57.
  27. Ponte AL, Marais E, Gallay N, et al. The in vitro migration capacity of human bone marrow mesenchymal stem cells: comparison of chemokine and growth factor chemotactic activities. *Stem Cells.* 2007;25:1737-1745.
  28. Zou C, Song G, Luo Q, Yuan L, Yang L. Mesenchymal stem cells require integrin beta1 for directed migration induced by osteopontin in vitro. *In Vitro Cell Dev Biol Anim.* 2011;47:241-250.
  29. Manfra DJ, Chen SC, Yang TY, et al. Leukocytes expressing green fluorescent protein as novel reagents for adoptive cell transfer and bone marrow transplantation studies. *Am J Pathol.* 2001;158:41-47.
  30. Grossniklaus HE, Ling JX, Wallace TM, et al. Macrophage and retinal pigment epithelium expression of angiogenic cytokines in choroidal neovascularization. *Mol Vis.* 2002;8:119-126.
  31. Kesen MR, Cousins SW. Choroidal neovascularization. In: Darlene AD, ed. *Encyclopedia of the Eye.* Oxford: Academic Press; 2010:257-265.
  32. Martin DF, Maguire MG, Ying GS, Grunwald JE, Fine SL, Jaffe GJ. Ranibizumab and bevacizumab for neovascular age-related macular degeneration. *N Engl J Med.* 2011;364:1897-1908.